

# Reconfigurable Beam-Steering Antenna Using Dipole and Loop Combined Structure for Wearable Applications

Sang-Jun Ha, Young-Bae Jung, Yongjin Kim, and Chang Won Jung

**This paper proposes a reconfigurable beam-steering antenna using a bended dipole and a loop. The radiation patterns of the two antennas are cancelled or compensated, and headed towards a specific direction when the dipole and loop antenna are combined at a reasonable ratio. The proposed antenna can steer the beam directions by controlling the operation of two artificial switches. The proposed antenna was manufactured on a PCB (FR-4) and a flexible PCB (polyimide). In the case of the antenna that was fabricated on a PCB, the maximum beam directions were  $+50^\circ$ ,  $0^\circ$ , and  $-50^\circ$  in the azimuth direction using the two artificial switches, and the antenna gain was 1.96 dBi to 2.48 dBi in the operation bandwidth of 2.47 GHz to 2.53 GHz. Also, the antenna was fabricated on a flexible PCB and measured under various bending conditions for wearable applications.**

**Keywords:** Reconfigurable antenna, dipole antenna, loop antenna, beam-steering, RF switches.

## I. Introduction

Wireless communication systems have been attempting to overcome the problem of limited channel bandwidth, satisfying a growing demand for a large number of mobile devices on communication channels [1], [2]. In several methods to improve the performance of such systems, beam switching can be used to enhance the spectral efficiency and reduce the problems associated with multipath propagation. Thus, the beam-steering antenna has been widely investigated [3]-[6]. It is capable of more strongly transmitting and receiving signals in the desired direction and preventing interference with other signals. Beam-steering antennas are mostly classified into adaptive array antenna using the phase shifter or single reconfigurable antenna using the switches [4]-[6]. The adaptive array antenna is used as the most common type of steerable antenna system and offers better gain than the single reconfigurable antenna. However, the size of the adaptive array antenna is bigger than that of the single reconfigurable antenna due to the use of multiple antenna elements and phase shifter. Recently, the size of the adaptive array antenna has to be reduced due to the space limitation in small mobile applications, such as EM sensors and note PCs [7], [8]. It is difficult to realize in those devices. Therefore, a single reconfigurable antenna with beam-steering capability is required for practical mobile applications.

In this paper, a reconfigurable beam-steering antenna that uses a folded dipole and a loop element is proposed. The structure of the proposed antenna is simple and planar. The antenna can steer the beam direction in the azimuth plane by

---

Manuscript received June 14, 2011; revised July 27, 2011; accepted Aug. 8, 2011.

This work was supported by the National Research Foundation of Korea with a grant from the Korean government (No. 2011-0005692).

Sang-Jun Ha (phone: +82 2 970 6803, hsj-913@nate.com) and Chang Won Jung (corresponding author, changwoj@snut.ac.kr) are with the Graduate School of NID Fusion Technology, Seoul National University of Science and Technology, Seoul, Rep. of Korea.

Young-Bae Jung (ybjung@hanbat.ac.kr) is with the Electronic Engineering Department, Hanbat National University, Daejeon, Rep. of Korea.

Yongjin Kim (yongjink@inhac.ac.kr) is with the Department of Electrical Information, Inha Technical College, Incheon, Rep. of Korea.

<http://dx.doi.org/10.4218/etrij.12.0111.0373>

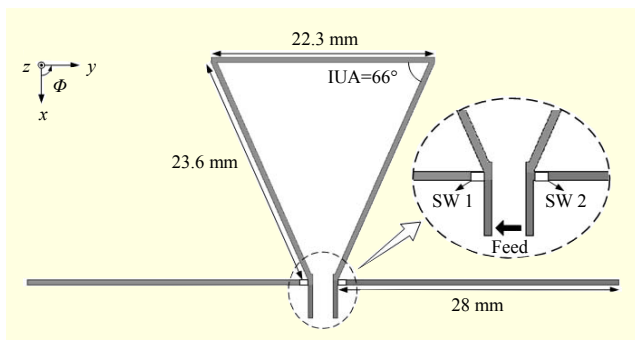


Fig. 1. Geometry of dipole and transformed loop combined antenna.

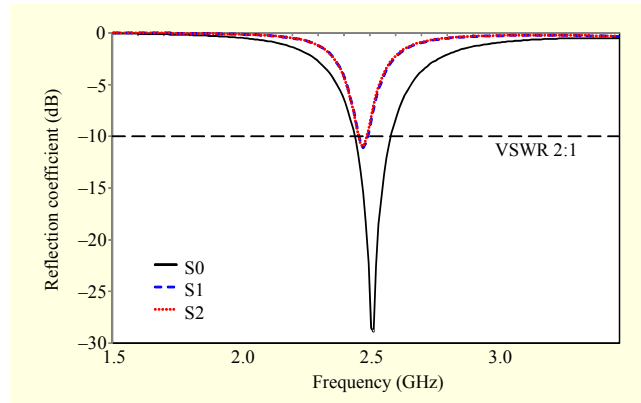


Fig. 2. Simulated reflection coefficients of antenna.

Table 1. Switch operation conditions.

State	Switch 1	Switch 2
S0	ON	ON
S1	ON	OFF
S2	OFF	ON

controlling the operation of the two switches. Moreover, the antenna performs well in a bending condition. Thus, this antenna structure can be widely used in a number of wearable applications such as the body area network (BAN), which requires antenna beam-steering capacity [9]-[12]. Ansoft's HFSS was used for the full wave analysis of the antenna.

## II. Proposed Antenna Design

The proposed antenna is composed of two radiating elements (a dipole and a loop). When the radiating elements are combined, the radiation patterns be cancelled or compensated for each other in a specific direction [13].

The antenna was designed to operate at 2.5 GHz. The length of the dipole is 28 mm, and the circumference of the loop is 69.5 mm as shown in Fig. 1. The dipole and loop elements were connected using two switches near the feed point. Two artificial switches were located between an input-port of the two radiating elements and can control their connection. There are three states in the configuration of the two artificial switches: S0, S1, and S2. S0 denotes that both switches 1 and 2 are in the ON-state. S1 denotes that only switch 1 is in the ON-state. S2 denotes that only switch 2 is in the ON-state. The switch in the ON-state means that the conductive line is connected between the indirect feed line and the antenna patch (short). Also, the switch in the OFF-state means that the conductive line was disconnected (open). The artificial switches make the ideal connection using a conductor. The

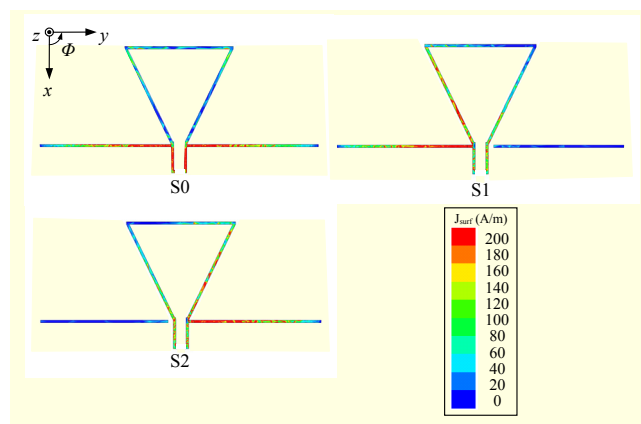


Fig. 3. Simulated surface current distribution on conductive part (S0, S1, and S2).

configuration of the three states is summarized in Table 1. To improve the performance of the reflection coefficient and the gain, the traditional circular loop was transformed into a triangular loop. When the included angle (IUA) of the triangle is about  $60^\circ$ , the input impedance matches it well at  $50 \Omega$  [14]. To make the resonant frequencies in all the switch operations identical at 2.5 GHz, the dipole element was transformed into the bended type. The inclined angle (IIA) is the bended angle of the dipole, and the maximum available angle is  $90^\circ$ . Figure 2 shows the simulated reflection coefficients of the states. The resonant frequencies of S1 and S2 are identical at 2.4 GHz, and that of S0 is 2.5 GHz. There is a 100-MHz difference between S0 and S1 and between S0 and S2. Figure 3 shows the simulated surface current distributions ( $J$  [A/m]) at each operation frequency. It is observed that the majority of the current distribution in the S0 is symmetrical. In S1, the current distributions are stronger on the left side of the antenna. Conversely, in S2, the current distributions are stronger on the right side. With this asymmetric current distribution of the asymmetric switch configurations of both S1 and S2, the maximum beam directions are tilted from the  $-y$  direction to

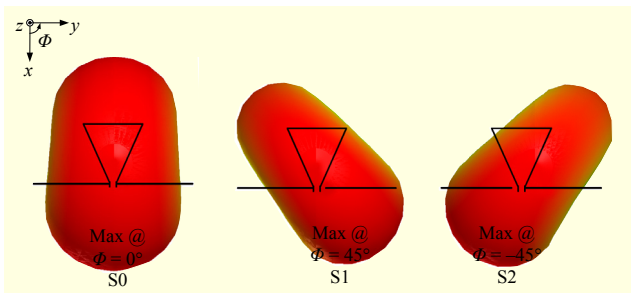


Fig. 4. Simulated radiation patterns of antenna at each resonant frequency ( $\theta = 90^\circ$  cut).

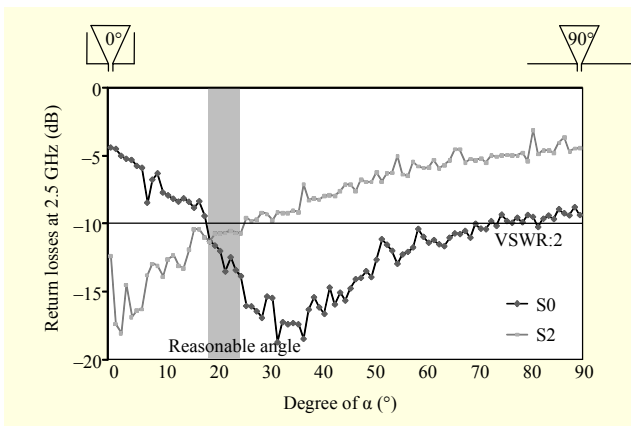


Fig. 5. Result of reflection coefficient versus inclined angle of folded dipole.

the  $+y$  direction. Figure 4 shows the simulated 3D radiation patterns ( $x$ - $y$  plane). The maximum beam directions were clearly changed by state (S0, S1, and S2). In S0, the maximum beam direction is in the  $x$  axis, at  $\Phi = 0^\circ$  and  $\theta = 90^\circ$ , and the gain at the maximum beam direction is 2.51 dBi. In S1, the maximum beam direction is  $\Phi = +45^\circ$  and  $\theta = 90^\circ$ , and the gain at the maximum beam direction is 1.07 dBi. In S2, the maximum beam direction is  $\Phi = -45^\circ$  and  $\theta = 90^\circ$ , and the gain at the maximum beam direction is 1.06 dBi. Figure 5 shows the simulated reflection coefficients of the S0 and S2 states according to the inclined angle of  $\alpha$  at 2.5 GHz. As the  $\alpha$  increases from  $0^\circ$  to  $40^\circ$ , the reflection coefficient of S0 improves, but the reflection coefficient of S2 is degraded. When  $\alpha$  is about  $19^\circ$  to  $26^\circ$ , the reflection coefficients of S0 and S2 are reasonably below  $-10$  dB in  $\text{VSWR} < 2$ . Therefore, it was decided that the optimum angle of  $\alpha$  is  $22^\circ$ . Figure 6 shows the antenna geometry for various break points of the dipole arm. The break point was investigated to optimize the antenna gain and input impedance. As a result of the simulation in Fig. 7, the break point is optimized and selected to 10 mm. At 10 mm of the break point, the reflection coefficients of both S0 and S2 satisfy with under  $-10$  dB, and gains of both S0 and S2 are higher than other break points. Figure 8 shows the

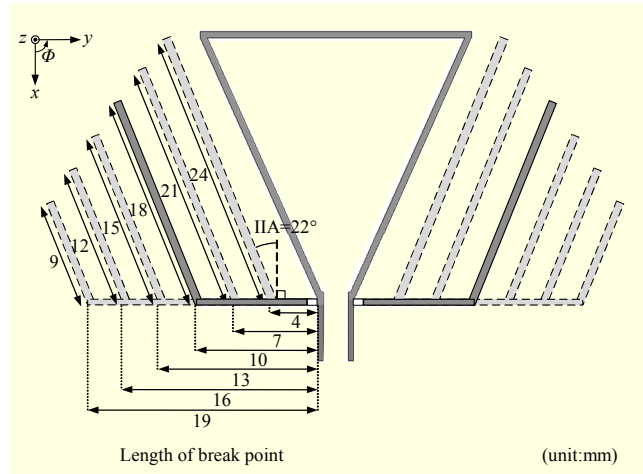


Fig. 6. Antenna geometry for various break points of dipole arm.

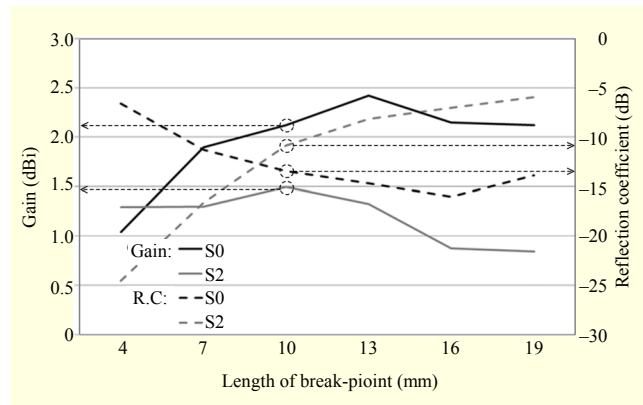


Fig. 7. Simulated reflection coefficients and gains for various break points of dipole arm.

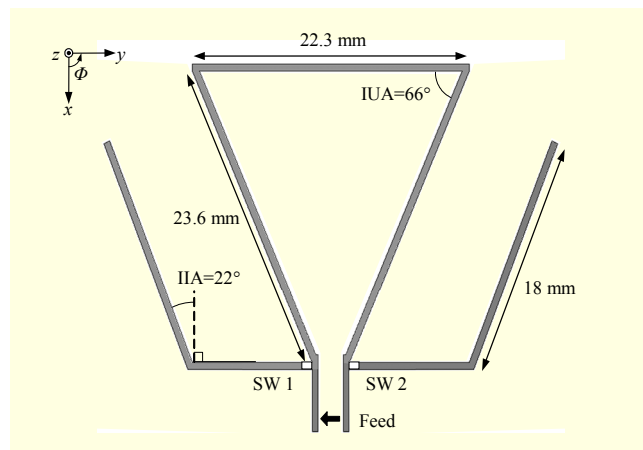


Fig. 8. Geometry of reconstructed antenna.

geometry of the reconstructed antenna. Figure 9 shows the simulated reflection coefficient when the optimum angle is  $22^\circ$ . The reflection coefficients of S0 and S2 in the optimum angle are  $-13.5$  dB and  $-10.8$  dB, respectively. Figure 10 shows the

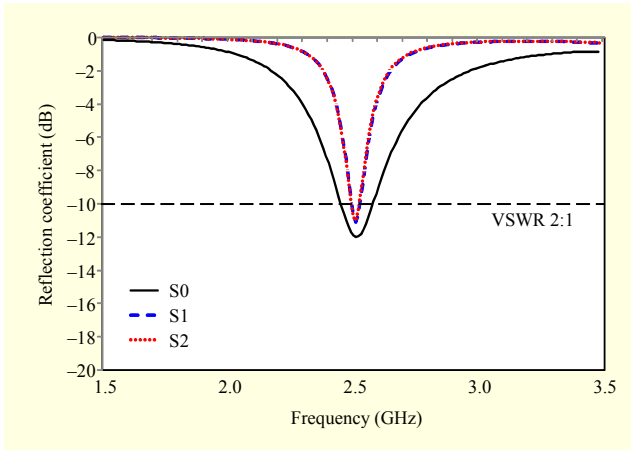


Fig. 9. Simulated reflection coefficient versus inclined angle of folded dipole.

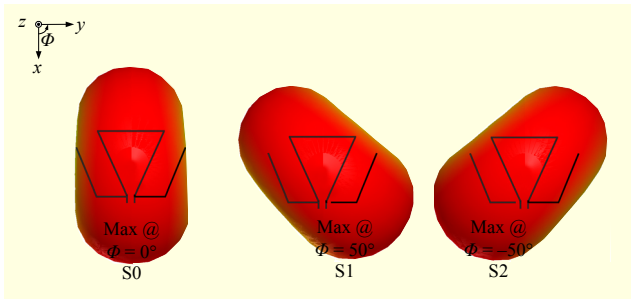


Fig. 10. Simulated radiation patterns of antenna with bended dipole at each resonant frequency ( $\theta = 90^\circ$  cut).

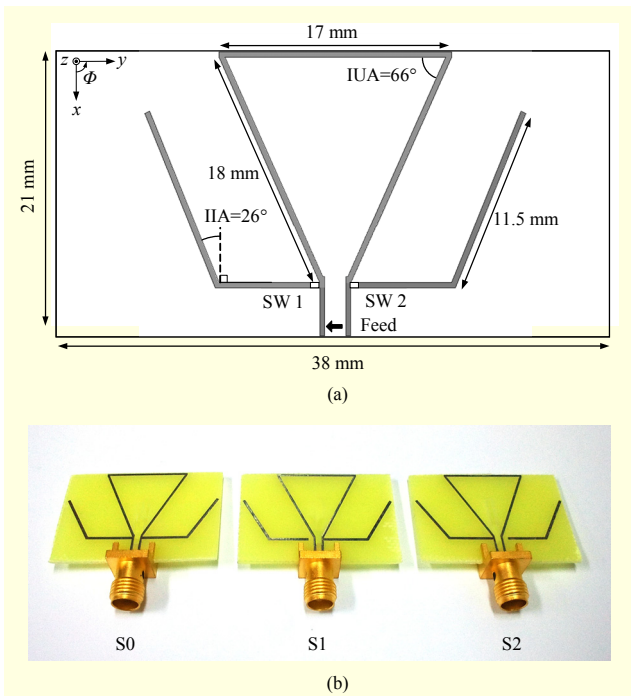


Fig. 11. (a) Geometry of proposed antenna fabricated on FR-4 and (b) photograph of antenna fabricated on FR-4.

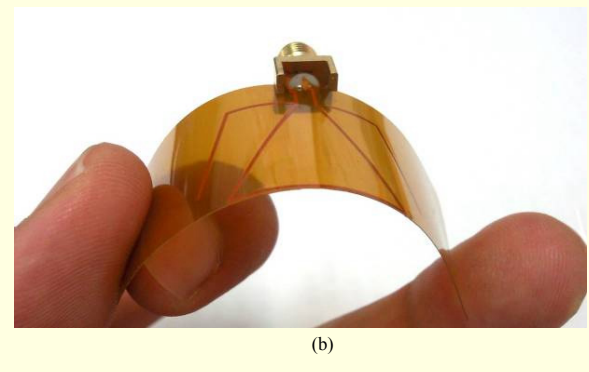
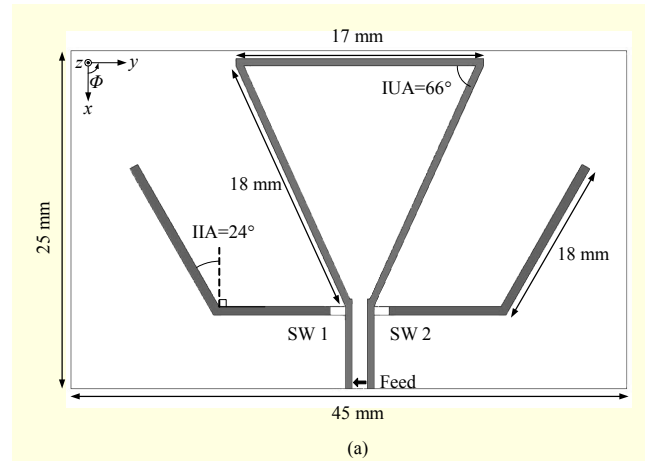


Fig. 12. (a) Geometry of proposed antenna fabricated on flexible PCB (polyimide) and (b) photograph of antenna fabricated on flexible PCB.

simulated 3D radiation patterns ( $x$ - $y$  plane). The maximum beam directions were clearly changed by state (S0, S1, and S2). In S0, the gain at the maximum beam direction is 2.35 dBi. In S1, the maximum beam direction is  $\Phi = +50^\circ$  and  $\theta = 90^\circ$ , and the gain at the maximum beam direction is 1.67 dBi. In S2, the maximum beam direction is  $\Phi = -50^\circ$  and  $\theta = 90^\circ$ , and the gain at the maximum beam direction is 1.66 dBi. Due to the reconstruction of  $\alpha$ , the resonant frequencies became identical and the maximum gains increased slightly. Figure 11 shows the geometry of the reconstructed antenna on a PCB ( $\epsilon_r = 4.4$  and  $\tan \delta = 0.02$ ). The antenna size is 38 mm  $\times$  21 mm, and its thickness is 1 mm. The top view of the proposed antenna that was fabricated on a flexible PCB ( $\epsilon_r = 3.6$  and  $\tan \delta = 0.01$ ) is shown in Fig. 12. The size of the antenna is 45 mm  $\times$  25 mm, and its thickness is 0.05 mm. This antenna was designed and fabricated to verify the antenna performance in the bending condition for wearable applications. Figure 13 shows a photograph of the proposed antenna under various bending conditions (R0, R1, and R2). R0 denotes that the antenna is physically flat, and R1 and R2 denote that the radii of the antenna are 30 mm and 15 mm, respectively.

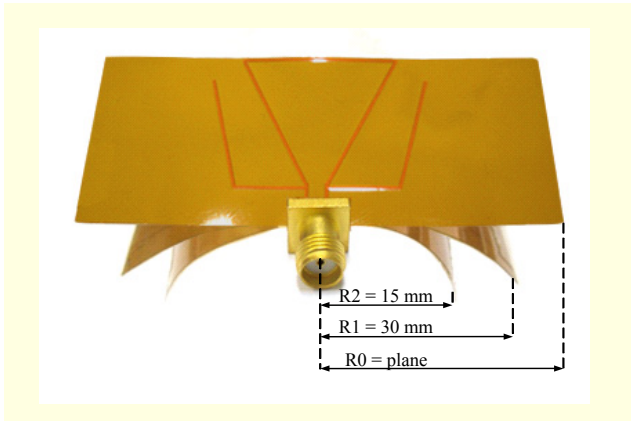


Fig. 13. Photograph of antenna fabricated on flexible PCB under various bending conditions.

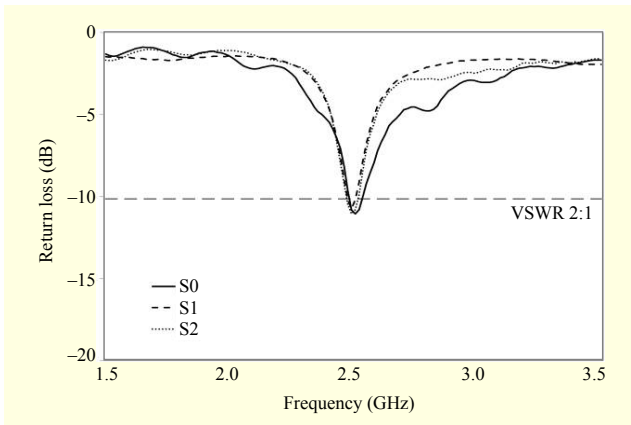


Fig. 14. Measured reflection coefficient of antenna fabricated on FR-4.

### III. Measurement Results and Discussion

#### 1. PCB (FR-4) Antenna Model

Figure 14 shows the reflection coefficient of the antenna that was fabricated on FR-4 according to the switch operation. As shown in this result, the resonance frequency was about 2.5 GHz for all states and the operation bandwidth was about 40 MHz to 60 MHz at  $VSWR < 2$ . Figure 15 shows the measured radiation patterns in the  $x$ - $y$  plane. From the result, a single beam was formed and the beam-pointing direction was clearly changed by the operation control of the switches. The radiation pattern of the antenna in the S0 state was similar to that of the conventional dipole with a maximum beam direction at  $180^\circ$ , a half-power beam width (HPBW) of  $80^\circ$ , and a gain at the maximum beam direction of 2.48 dBi. In the S1 state, the maximum beam direction was  $130^\circ$ , HPBW was  $100^\circ$ , and the gain at the maximum beam direction was 2.11 dBi. Also, in the S2 state, the antenna had a maximum beam direction of  $230^\circ$  with  $HPBW = 100^\circ$ , and the gain at the maximum beam direction was 1.96 dBi, which

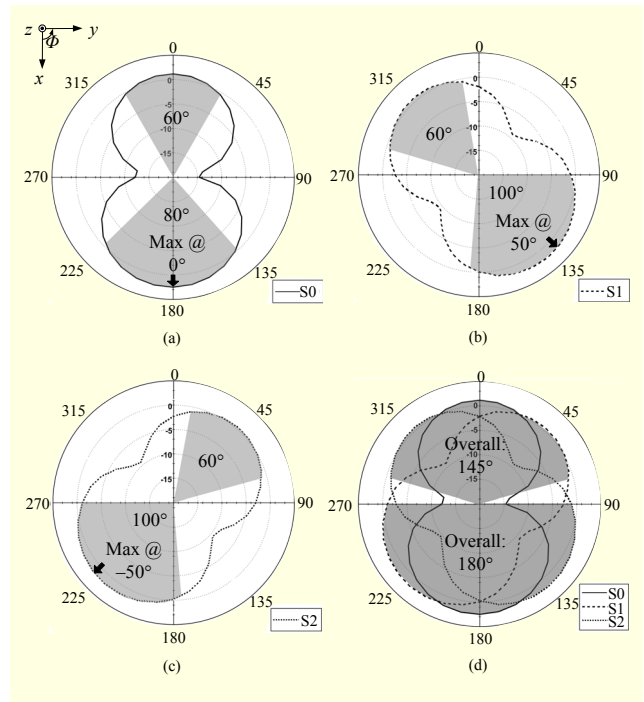


Fig. 15. Measured radiation patterns of antenna fabricated on FR-4 at 2.5 GHz ( $\theta = 90^\circ$  cut): (a) S0, (b) S1, (c) S2, and (d) overall HPBW.

is exactly symmetrical with the S1 state. The overall HPBW for the three states was  $180^\circ$ .

#### 2. Flexible PCB (Polyimide) Antenna Model

Figure 16 shows the measured reflection coefficients of the antenna that was fabricated on a flexible PCB in the bending conditions of R0, R1, and R2. The reflection coefficients were almost not influenced by the bending conditions. The operation frequencies of the antenna in the switch operation states and the bending conditions were same at the operation frequency of 2.5 GHz, and the operation bandwidth was about 40 MHz to 60 MHz at  $VSWR < 2$ . Figure 17 shows the measured radiation patterns in the  $x$ - $y$  plane. The radiation pattern of the antenna in the S0 state was similar to that of the conventional dipole that also had a maximum beam direction of  $180^\circ$ , an HPBW of  $80^\circ$ , and a gain at the maximum beam direction of 1.6 dBi. In the S1 state, the maximum beam direction was  $130^\circ$ , the HPBW was  $100^\circ$ , and the gain at the maximum beam direction was 1.4 dBi. Also, in the S2 state, the maximum beam direction was  $230^\circ$  with an HPBW of  $100^\circ$ , and the gain at the maximum beam direction was 1.5 dBi. This direction is symmetrical with that at the S1 state. The overall HPBW for the steering beam was  $180^\circ$ . Figure 18 shows the measured 3D radiation patterns under various bending and switch operation conditions. The overall gain of the nine states was 0.8 dBi to



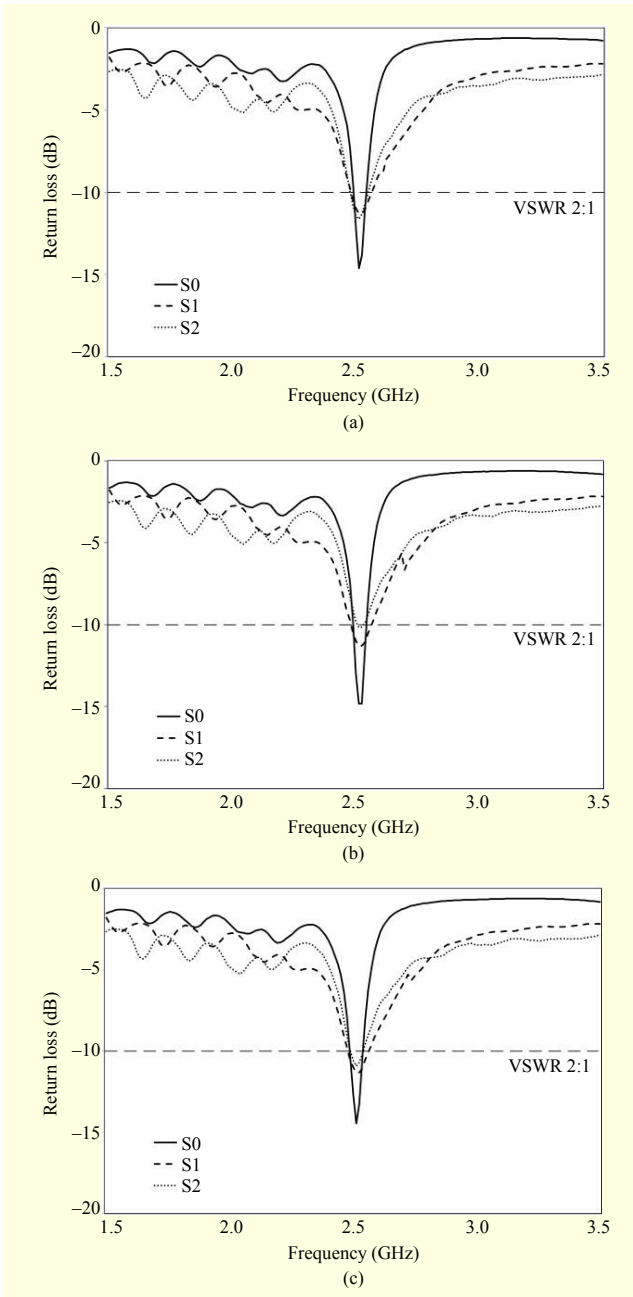


Fig. 16. Measured reflection coefficient of antenna fabricated on flexible PCB: (a) R0, (b) R1, and (c) R2.

1.6 dBi, and their HPBW was  $86^\circ$  to  $111^\circ$ , respectively. The maximum beam-steering angle of the S1 and S2 states was  $18^\circ$  to  $50^\circ$ , respectively. The maximum beam directions of the S0 state in all bending conditions were identical to  $0^\circ$  in the azimuth plane, and the peak gain was 0.9 dBi to  $-1.5$  dBi, with an HPBW of  $81^\circ$  to  $109^\circ$ , respectively. The maximum beam-steering angles of the S1 and S2 states are exactly symmetrical to each other in the R0, R1, and R2 states, and the beam tilt angles of the S1 and S2 states decreased as the radius decreased. The detailed measurement results for the flexible antenna

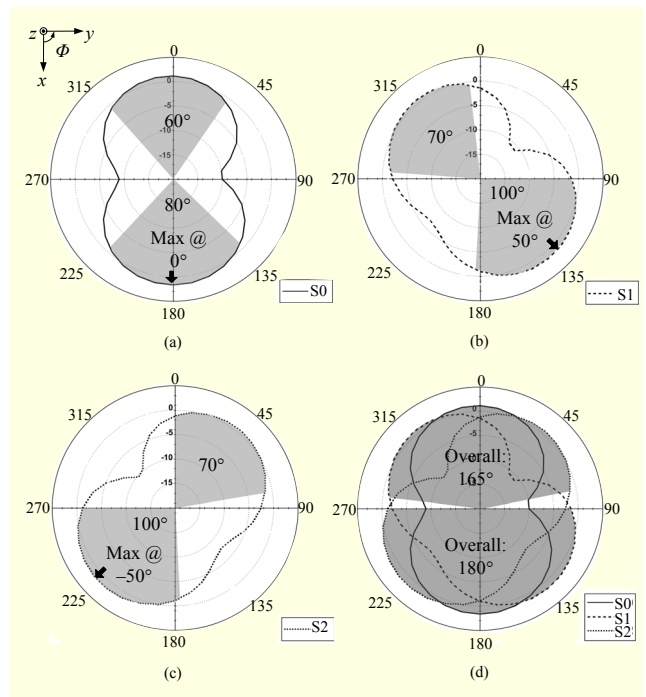


Fig. 17. Measured radiation patterns of antenna fabricated on flexible PCB at 2.5 GHz ( $\theta = 90^\circ$  cut): (a) S0, (b) S1, (c) S2, and (d) overall HPBW.

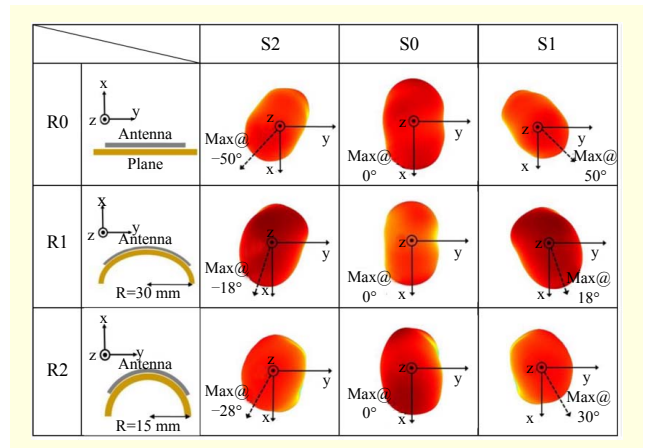


Fig. 18. Measured radiation 3D patterns of antenna fabricated on flexible PCB at 2.5 GHz ( $\theta = 90^\circ$  cut).

model are summarized in Table 2. When we measured the proposed antenna, a standard 4:1 transmitting balun was used to adapt an unbalanced device to a balanced one [15]. In future work, we are going to design an antenna with a CPW feed line and ground plane for real RF switch use. The bias circuit using two PIN diodes is shown in Fig. 19. The forward bias voltage (DC1 and DC2) to the PIN diodes can be switched between 0 V and 1 V to operate the antenna [16]. Two inductors are connected to the folded dipole as RF chokes. In the measurement, the bias tee is used at the feed point to

**Table 2.** Detailed results of measurements of antenna fabricated on flexible PCB.

States		Max. beam direction (°)		Peak gain (dBi)	HPBW (°)
		$\Phi$	$\theta$		
R0 (plane)	S0	0	90	1.6	66
	S1	+50	90	1.4	70
	S2	-50	90	1.5	65
R1 (R = 30 mm)	S0	0	95	0.9	108
	S1	+30	100	0.8	111
	S2	-28	98	1.0	109
R2 (R = 15 mm)	S0	0	102	1.4	103
	S1	+18	103	1.5	98
	S2	-18	102	1.4	101

**Table 3.** Switch operation conditions.

State	DC1	DC2
S0	1 V	1 V
S1	1 V	0 V
S2	0 V	1 V

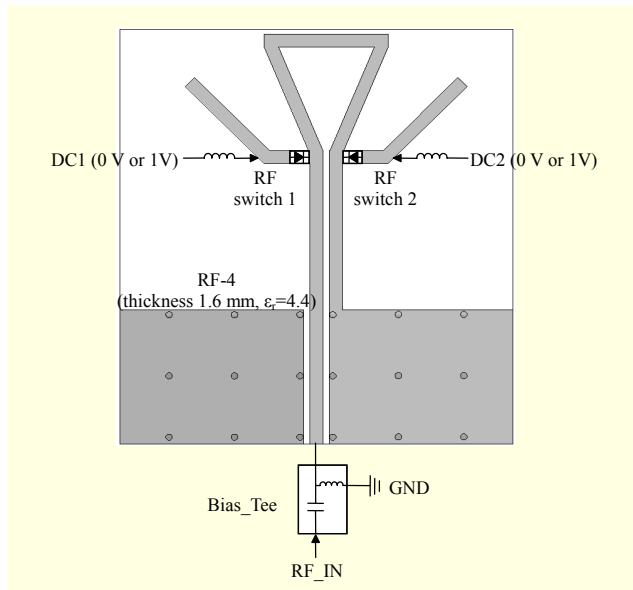


**Fig. 19.** Configuration of bias circuit using RF switches.

block DC current and to transmit RF input signal [16]. Table 3 shows the conditions of two switch operations by the applied voltage (DC1 and DC2).

#### IV. Conclusion

In this paper, a reconfigurable beam-steering antenna using a

dipole and a loop element was designed and analyzed. The proposed antenna structure is simple and easy to fabricate. From the measurement results, it was confirmed that the proposed antenna structure very effectively realizes the antenna beam-steering capacity with switch operation and performs well in various bending conditions in a conformal size. Thus, the proposed antenna is a candidate for various wearable applications and can be applicable to a communication system that requires antenna beam-steering capacity.

#### References

- [1] A. Alexiou and M. Haardt, "Smart Antenna Technologies for Future Wireless Systems: Trends and Challenges," *IEEE Commun. Mag.*, vol. 42, no. 9, Sept. 2004, pp. 90-97.
- [2] M. Chryssomallis, "Smart Antennas," *IEEE Antennas Propag. Mag.*, vol. 42, no. 3, June 2000, pp. 129-136.
- [3] S. Yan and T. Chu, "A Beam-Steering and Switching Antenna Array Using a Coupled Phase-Locked Loop Array," *IEEE Trans. Antennas Propag.*, vol. 57, no. 3, Mar. 2009, pp. 638-644.
- [4] P. Deo et al., "Thickness Reduction and Performance Enhancement of Steerable Square Loop Antenna Using Hybrid High Impedance Surface," *IEEE Trans. Antennas Propag.*, vol. 58, no. 5, May 2010, pp. 1477-1485.
- [5] C.W. Jung et al., "Reconfigurable Scan-Beam Single-Arm Spiral Antenna Integrated with RF-MEMS Switches," *IEEE Trans. Antennas Propag.*, vol. 54, no. 2, Feb. 2006, pp. 455-463.
- [6] G.H. Huff and J.T. Bernhard, "Integration of Packaged RF MEMS Switches with Radiation Pattern Reconfigurable Square Spiral Microstrip Antennas," *IEEE Trans. Antennas Propag.*, vol. 54, no. 2, Feb. 2006, pp. 464-469.
- [7] M.-I. Lai et al., "Compact Switched-Beam Antenna Employing a Four-Element Slot Antenna Array for Digital Home Applications," *IEEE Trans. Antennas Propag.*, vol. 56, no. 9, Sept. 2008, pp. 2929-2936.
- [8] C.-J. Wang and W.-T. Tsai, "A Slot Antenna Module for Switchable Radiation Patterns" *IEEE Antennas Wireless Propag. Lett.*, vol. 4, June 2005, pp. 202-204.
- [9] C. Hertleer et al., "Aperture-Coupled Patch Antenna for Integration into Wearable Textile Systems," *IEEE Antennas Wireless Propag. Lett.*, vol. 6, June 2007, pp. 392-395.
- [10] S. Zhu and R.J. Langley, "Dual-Band Wearable Textile Antennas on an EBG Substrate," *IEEE Trans. Antennas Propag.*, vol. 57, no. 4, Apr. 2009, pp. 926-935.
- [11] M. Klemm and G. Troester, "Textile UWB Antennas for Wireless Body Area Networks," *IEEE Trans. Antennas Propag.*, vol. 54, no. 11, Nov. 2006, pp. 3192-3197.
- [12] M. Tanaka and J. Jang, "Wearable Microstrip Antenna," *IEEE Antennas Propag. Soc. Int. Symp.*, vol. 2, no. 22, June 2003, pp. 704-707.

- [13] D.H. Kwon, "On the Radiation Q and the Gain of Crossed Electric and Magnetic Dipole Moment," *IEEE Trans. Antennas Propaga.*, vol. 53, no. 5, May 2005, pp. 1681-1687.
- [14] C.A. Balanis, *Antenna Theory Analysis and Design*, 2nd ed., New York: John Wiley & Sons, 2001.
- [15] O.M. Woodward, "Balance Measurements on Balun Transformers," *Electron.*, Sept. 1953, pp. 188-191.
- [16] C.W. Jung et al., "Macro-Micro Frequency Tuning Antenna for Reconfigurable Wireless Communication Systems," *Electron. Lett.*, vol. 43, no. 4, Feb. 2007, pp. 201-202.



**Sang-Jun Ha** received the BS in media engineering from Seoul National University of Science and Technology, Seoul, Rep. Of Korea, in February 2010. Since March 2010, he has been with the Graduate School of Nano-IT-Design (NID) Fusion Technology, Seoul National University of Science and Technology.

His current research is focussed on beam reconfigurable antennas and wearable applications.



**Young-Bae Jung** received the BS in radio science and engineering from Kwangwoon University, Seoul, Rep. of Korea, in 1999, the MS and PhD in information and communications engineering from Korea Advanced Institute of Science and Technology (KAIST), Daejeon, Rep. of Korea, in 2001 and

2009, respectively. From 2001 to 2011, he was with ETRI, Daejeon, Rep. of Korea, as a senior researcher. Since March 2011, he has been a professor with the Department of Electric, Electronic and Control Engineering, Hanbat National University, Daejeon, Rep. of Korea. His work is focused on active phased array antenna systems and next generation mobile base-station antennas. His research interests include active phased array antenna systems and active/passive components in the field of RF and microwave.



**Yongjin Kim** received the BS in electrical engineering from Inha University, Incheon, Rep. of Korea, in 1992, and the MS and PhD in electrical engineering from Ohio State University, Columbus, USA, in 1999 and 2003, respectively. After his graduate work at the Electro Science Laboratory (ESL), he joined the

Samsung Advanced Institute of Technology, Yongin, Rep. of Korea, as a senior research engineer. Currently, he is an assistant professor in the Department of Electrical Information at Inha Technical College, Rep. of Korea. His research interests includes antenna design and optimization technology for modern communication services, such as UWB, RFID, cellular, DMB/DVB-H, and MIMO systems.



**Chang Won Jung** received the BS in radio science and engineering from Kwangwoon University, Rep. of Korea, in 1997, the MS in electrical engineering from University of Southern California (USC), Los Angeles, USA, in 2001, and the PhD in electrical engineering and computer sciences from the University of

California, Irvine (UCI), USA, in June 2005. From 1997 to 1999, he joined LG Information and Telecommunication in Korea, as a research engineer in the wireless communication field. Also, from 2005 to 2008, he was senior research engineer in Samsung Advanced Institute of Technology (SAIT), Rep. of Korea. Since 2008, he has been with the Graduate School of Nano-IT-Design (NID) Fusion Technology, Seoul National University of Science and Technology (SNUST), as an assistant professor. His current research interests are antennas for MMMB communication systems, multifunctional reconfigurable antennas, EMI/ EMC, millimeter wave applications, and metamaterial technology, including frequency selective surface (FSS).